Journal of Nuclear Materials 390–391 (2009) 290–294

Contents lists available at ScienceDirect

Journal of Nuclear Materials

journal homepage: www.elsevier.com/locate/jnucmat

Investigation of detached recombining deuterium plasma and carbon chemical erosion in the toroidal divertor simulator NAGDIS-T

K. Yada [a], N. Matsui [a], N. Ohno [a,*], S. Kajita [b], S. Takamura [c], M. Takagi [a]

[a] Department of Energy Engineering and Science, Nagoya University, Furo-cho, Chikusa-ku, Nagoya 464-8603, Japan
[b] EcoTopia Science Institute, Nagoya University, Furo-cho, Chikusa-ku, Nagoya 464-8603, Japan
[c] Department of Electronics, Aichi Institute of Technology, Yakusa-cho, Toyota 470-0392, Japan

ARTICLE INFO

PACS:
52.25.−b
52.40.Hf

ABSTRACT

Detached deuterium recombining plasma has been generated in the toroidal divertor simulator. The electron temperature (0.1–0.4 eV) and density ($\sim 10^{18}$ m^{-3}) in the detached plasmas were evaluated with a spectroscopic method using a series of deuterium Balmer line emission from highly excited levels and the Stark broadening of D(2–12). We have investigated the role of volume plasma recombination through Electron–Ion Recombination (EIR) and Molecular Activated Recombination (MAR) processes. Moreover, the carbon erosion in the detached deuterium plasma has been studied with a weight loss method. It is found that deuterium neutrals generated by EIR process could have strong influence on the carbon chemical erosion.

1. Introduction

Linear divertor plasma simulators (L-DPS) have contributed to understand edge plasma physics and plasma-wall interaction in fusion devices [1]. However, L-DPS cannot simulate some important phenomena in scrape-off layer (SOL) and divertor region, for example non-diffusive plasma transport, which is driven by gradient and curvature of magnetic field, and plasma-wall interaction associated with grazing incident magnetic field line. To conduct comprehensive studies of SOL plasma physics, we have developed the toroidal divertor plasma simulator NAGDIS-T (NAGoya DIvertor plasma Simulator with Toroidal magnetic configuration) [2], which can generate deuterium plasmas with an electron density above of 10^{19} m^{-3} in steady state. Although the plasma parameters in the NAGDIS-T is not sufficient to simulate the divertor conditions, particularly, those in ELMy H-mode of tokamaks, NAGDIS-T can demonstrate important phenomena in the divertor region, such as plasma detachment and so on.

Plasma detachment is thought to be an effective method to reduce the heat load to the plasma facing components. Extensive studies concerning the plasma detachment have been performed in L-DPS [3,4] and fusion devices [5–7]. However, open questions still remain concerning the roles of Molecular Activated Recombination (MAR) compared with Electron–Ion Recombination (EIR) including radiative and three body recombination, and the roles of non-diffusive plasma transport in the detached plasma [8–11]. EIR requires very low electron temperatures (less than ~0.5 eV) to be effective. On the other hand, MAR was proposed as an alternative recombination mechanism in a relatively high electron temperature range. Although the reaction channels in MAR are known, MAR has not yet been shown to be dominant in fusion devices. Another important issue is the chemical erosion of graphite in detached deuterium plasma. Although physical sputtering yield decreases in detached plasmas because the electron temperature, namely, the incident ion energy, is sufficiently low, the chemical erosion due to the low energy deuterium ions and atoms generated by recombining process may be enhanced. At present, however, the chemical erosion of graphite in detached deuterium plasmas is not fully understood yet [12,13].

In the NAGDIS-T, we can produce detached deuterium plasmas in steady state by controlling neutral pressure. In the present paper, the characteristics of detached plasmas are investigated by using Langmuir probe and spectroscopic methods. By controlling plasma parameters, we will demonstrate the transition from the EIR-dominating condition to the MAR-dominating one. We also study the chemical erosion of graphite in the detached deuterium plasma, which is one of the most important issues to estimate the lifetime of carbon in fusion devices.

2. Experimental setup

The NAGDIS-T consists of 12 toroidal magnetic field coils and four vertical field coils, as shown in Fig. 1(a). These coils can produce a helical magnetic configuration. The major radius is 0.34 m

* Corresponding author.
E-mail addresses: k-yada@ees.nagoya-u.ac.jp (K. Yada), ohno@ees.nagoya-u.ac.jp (N. Ohno).

0022-3115/$ - see front matter © 2009 Elsevier B.V. All rights reserved.
doi:10.1016/j.jnucmat.2009.01.123

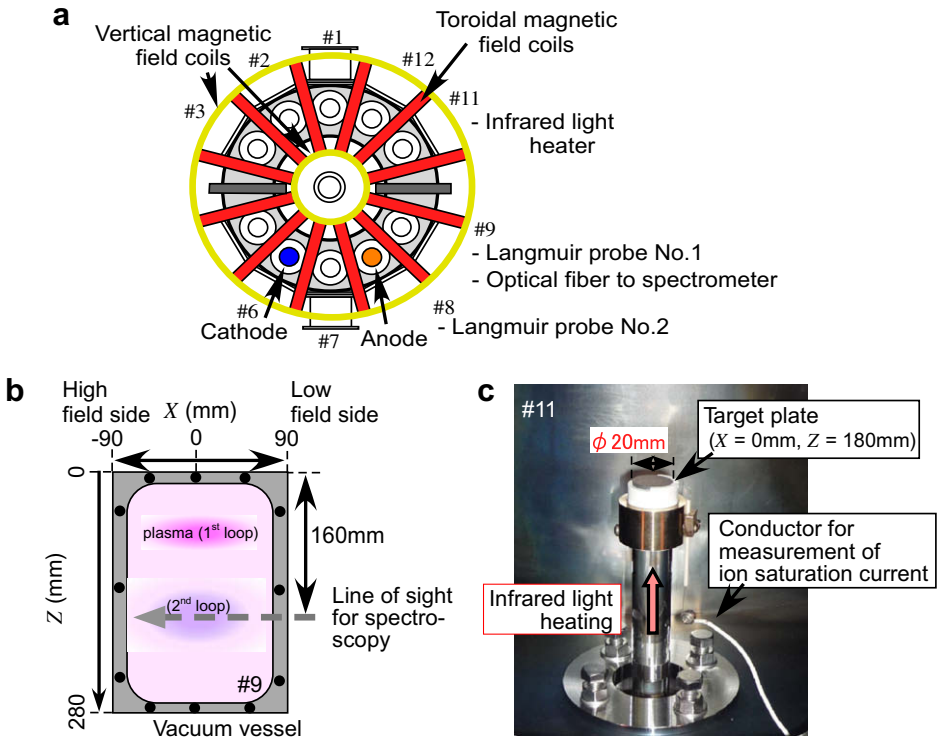

Fig. 1. Schematic diagram of the toroidal divertor plasma simulator NAGDIS-T. (a) The top view, (b) poloidal cross section and (c) photograph of the experimental set up for plasma irradiation experiments.

and the poloidal cross section of the vacuum chamber has a rectangular shape with a vertical height of 0.28 m and horizontal width of 0.18 m, as shown in Fig. 1(b). The toroidal magnetic field, B_t, and vertical magnetic field, B_v, are, respectively, $\leqslant$0.1 T and 3.0×10^{-3} T at the center of the vacuum vessel. The magnetic field line, which starts from the top surface of the vacuum chamber, goes down rotating toroidally. The incident angle of the magnetic field line to the target plate and the connection length L can be controlled from 40 m to 300 m by changing the ratio of the vertical and the toroidal magnetic field strengths. The cathode is made of LaB_6, which is heated up to 1700 K by DC Joule heating [14].

Langmuir probe No. 1, which is equipped at the upper port of section #9, is used to measure the 2-D plasma parameters in attached plasma condition. Moving range of this probe is horizontally 50 mm and vertically 180 mm. Additionally, probe No. 2, which is movable in the radial direction, is also set at the side port of section #8. In detached plasmas, plasma parameters are evaluated with optical methods because it was reported that the anomaly of the probe characteristics appears in detached condition [15,16]. Note that the ion saturation current is reliable even in the detached plasmas. The spectra of visible light emissions are measured at section #9 (Fig. 1(a)). A 0.75-m Czerny-Turner spectrograph with 1800 grooves/mm grating is used for spectroscopy. The instrumental width is 0.011 nm and the wavelength cover range is 300–700 nm. The emission from the plasma was collected by an optical lens, the diameter and focal length of which are both 50 mm, and coupled into an optical fiber. The diameter of the fiber core is 230 μm and image of the optical fiber is at the center of the vacuum chamber 1.2 mm, which is much less than the width of plasma column.

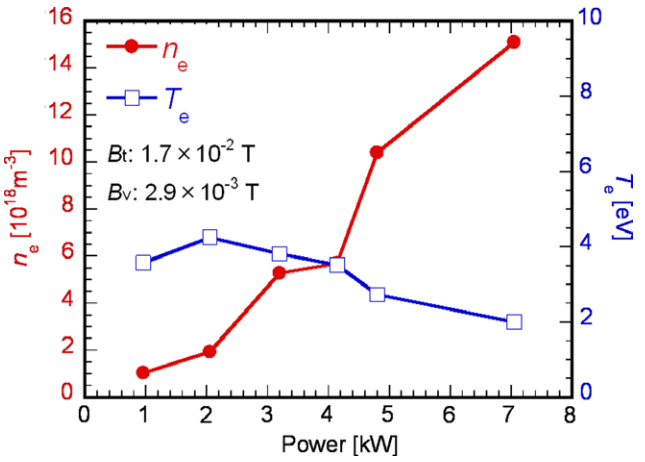

Fig. 2. Discharge power dependence of electron density n_e (circles) and temperature T_e (squares) at the position where the distance from the cathode is 0.36 m.

3. Experimental results

3.1. Generation of deuterium plasmas

Fig. 2 shows a DC discharge power dependence of plasma density n_e and temperature T_e measured by the Langmuir probe No. 2 at $X = 0$ mm and $Z = 50$ mm, where X is the horizontal position from the center of the vacuum vessel, and Z is the vertical one from the top of the vessel in Fig. 1(b). As shown in Fig. 2, the deuterium plasma with $n_e \sim 1.5 \times 10^{19}$ m^{-3} and $T_e \sim 2$ eV is generated at a discharge power of 7 kW. Fig. 3(a) shows a typical photograph of a deuterium plasma in the attached condition at a neutral pressure of 7.8×10^{-2} Pa. We can clearly observe a deuterium plasma with spiral shape. The deuterium plasma generated at the top is transported along the open helical magnetic field because the parallel transport along the field line is much faster than the cross-field

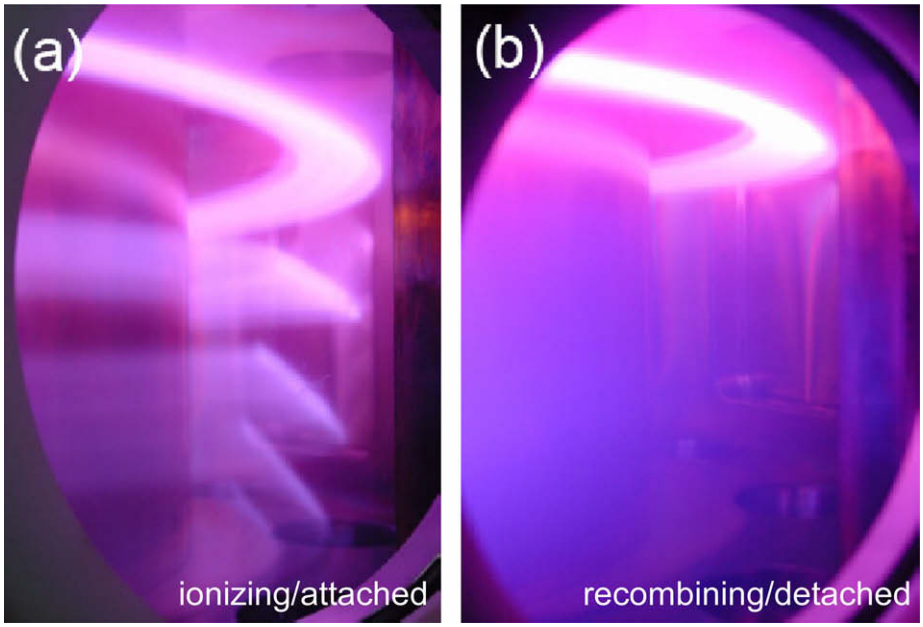

Fig. 3. Typical photograph of (a) the attached plasma and (b) the detached plasma.

plasma transport. It is noted that the 2nd loop of the spiral plasma shifts inward, and finally the 5th loop reaches the side chamber wall of the vacuum vessel at high field side. Fig. 4(a) shows a 2-D distribution of n_e measured with Langmuir probe No. 1. Here, the positive X corresponds to the low field side direction, and the inner/outer walls are located at $X = -90/90$ mm. The vertical and horizontal step sizes of the measurement are 4 mm and 5 mm, respectively. The horizontal profiles of n_e at the 1st (44 mm < Z < 52 mm) and the 2nd (116 mm < Z < 124 mm) loops are shown in Fig. 4(b). It is found that the plasma shifts toward the high field side. We performed the same experiments by changing B_t and B_v, however, the inward shift does not change. At present, the mechanism of the plasma shifts has not been understood yet.

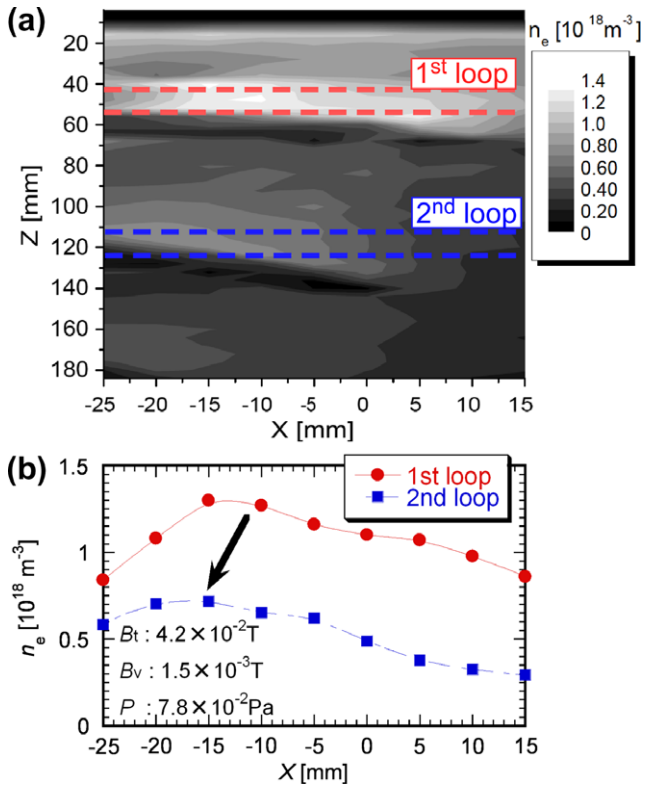

Fig. 4. (a) 2-D distribution of electron density in the case of the attached plasma and (b) horizontal profiles of the electron density at 1st and 2nd loops.

3.2. Overview of detached deuterium plasma

Fig. 3(b) is a typical photograph showing the formation of the plasma detachment. The neutral pressure P was 0.56 Pa. The spectra observed from the 1st and the 2nd loop of spiral plasma are shown in Fig. 5(a) and (b), respectively. At spectrum at the 1st loop, visible line emissions from electrically excited hydrogen molecules as well as Balmer series are observed due to electron impact excitation. On the other hand, at the 2nd loop, the series of visible line emissions from highly excited levels, which are an indicator of three body recombination process, were clearly observed in Fig. 5(b).

The partial local thermodynamic equilibrium is satisfied above a certain quantum number n_{cr} [17], which is ~5 in a typical detached plasmas ($n_e \sim 10^{18}$ m^{-3}, 0.1 eV < T_e < 0.5 eV); thus, we evaluated T_e by Boltzmann plot method with using the emission from $n = 7$–14 [18]. Fig. 5(c) shows the relative population densities divided by the statistical weight; the slope gives T_e of 0.11 eV. Additionally, n_e is evaluated from the Stark broadening of D(2–12) [17]. In case of Fig. 5(b), the Stark width of $\Delta\lambda(2\text{–}12) = 0.038$ nm, which is obtained by considering the instrumental width of 0.011 nm, gives the electron density of 3.3×10^{18} m^{-3}. The effects of the Doppler broadening (0.006 nm at a neutral temperature of 0.1 eV) and Zeeman splitting [19] are negligible. The experimental results indicate that EIR plays the dominant role for the formation of the detached deuterium plasma when T_e is less than 0.5 eV.

3.3. Transition between EIR and MAR in detached deuterium plasma

In Fig. 6(a), the emission intensity D(2–7) and the ratio to D_α at the 2nd loop plasma are plotted against the electron density at the 1st loop, which is measured with the probe No. 1. The neutral pressure is 0.59 Pa, and the magnetic field strengths are

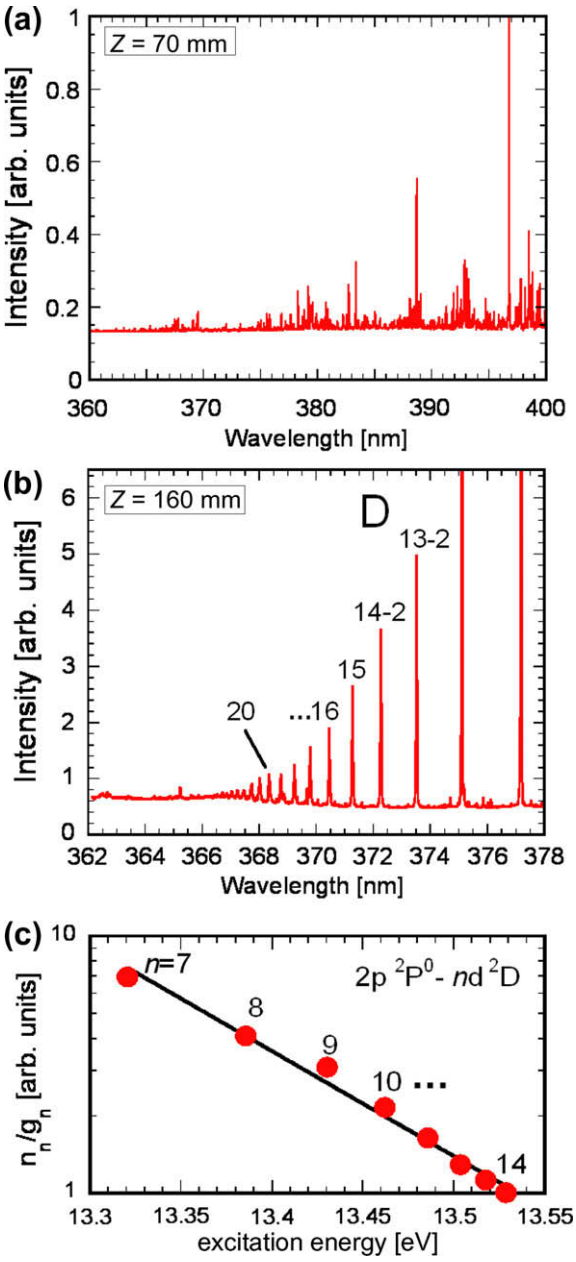

Fig. 5. Series of deuterium Balmer spectrum (a) at the 1st loop (b) at the 2nd loop where the neutral pressure was 0.56 Pa. Inset shows the enlargement of the spectrum at highly excited states. (c) Population density of n states per statistical weight as a function of excitation energy from the ground state.

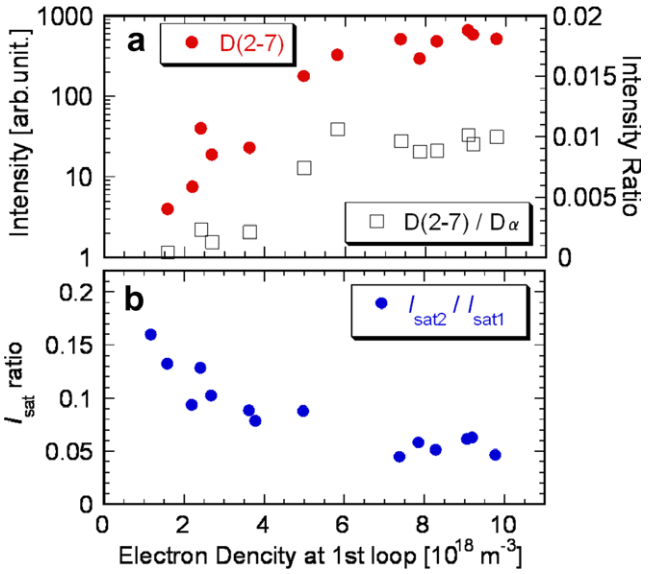

Fig. 6. (a) Emission intensity of D(2–7) lines (closed circles) and the intensity ratio of D(2–7) and D_α (open squares), (b) The ion saturation current ratio of 1st loop plasma and 2nd loop as a function of the electron density at 1st loop plasma.

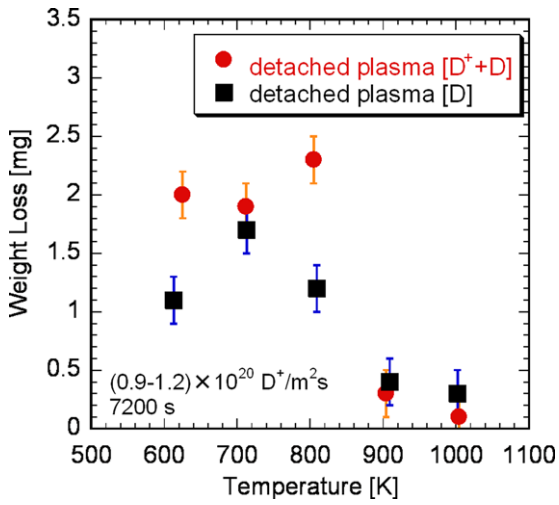

Fig. 7. Surface temperature dependence of weight loss by detached deuterium plasma irradiation.

$B_t \sim 3.0 \times 10^{-2}$ T and $B_v \sim 1.8 \times 10^{-3}$ T. When the electron temperature is less than 1 eV, the electron impact excitation from the ground state to $n = 7$ rarely occurs. Thus, the population densities at highly excited states are determined by the EIR process. Since D(2–7) emission is proportional to the population density at $n = 7$, it can be used as an indicator of EIR process. Fig. 6(b) shows the n_e dependence of the ratio of I_{sat2} to I_{sat1}, where I_{sat2} and I_{sat1} are the ion saturation current in the 2nd loop (measured with probe No. 2) and the 1st one (measured with probe No. 1), respectively.

The ratio D(2–7)/D_α significantly decreases as decreasing n_e, when n_e is around 5×10^{18} m^{-3}. This indicates that effect of EIR becomes weak in the low density region. In fact, the series of spectral lines from highly excited states almost disappears. Although the EIR almost disappears below $n_e \sim 5 \times 10^{18}$ m^{-3}, the normalized ion saturation currents I_{sat2}/I_{sat1} are approximately 0.15 which is still small. In the attached plasma, at which $P \sim 8.4 \times 10^{-2}$ Pa, $B_t = 3.0 \times 10^{-2}$ T, and $B_v = 1.8 \times 10^{-3}$ T, I_{sat2}/I_{sat1} was ~0.6, which is significantly larger than that in the detached plasma. Therefore, the plasma particles are lost due to not only the EIR processes but also other processes, and MAR could be an plasma particle loss channel. In Fig. 6(a), in addition to the decrease of the effect of the EIR, there is a possibility that the population density at $n = 3$ is selectively increased owing to MAR process [8,20] in the low density region. We believe that MAR coexists with EIR in deuterium plasma under the present experimental condition.

3.4. Chemical erosion experiment of carbon in detached deuterium plasma

High grade isotropic graphite target plate (ETP10, IBIDEN Co. Ltd.) of 20 mm in diameter and 2 mm in thickness was installed at the position along the magnetic field from the cathode. Fig. 1(c) shows the photograph of the experimental setup. The

weight loss method with an accuracy of ±0.1 mg is used for the determination of the eroded weight. The surface temperature of the graphite target was controlled externally with an infrared light heater equipped at the lower port of #11, and was monitored by using an IR-pyrometer calibrated with a thermocouple. The graphite target was exposed to the detached deuterium plasma for 7200 s. The electron density and temperature were 1.7×10^{18} m^{-3} and 0.12 eV, respectively.

Surface temperature dependence of the weight loss of graphite target is shown in Fig. 7. Closed circles show the weight losses when the target is at the floating potential. In this case, both ions and neutrals are bombarded to the graphite target. The ion flux Γ evaluated from the ion saturation current to the target is $(0.9–1.2) \times 10^{20}$ D^+/m^{2}s. The ion incident energy is less than 1 eV because the incident ion energy is determined by the sheath voltage, and the sheath voltage can be estimated to be about 0.4 eV at an electron temperature of 0.12 eV for a deuterium plasma.

Under detached plasma condition, since the electron density is high and the electron temperature is low, heat exchange time between electrons and ions is quite short [21]. Thus, the ion temperature is close to the electron one. The temperature of deuterium neutral generated by EIR process is same as ion temperature of ~0.1 eV. Therefore, the physical sputtering of graphite target due to deuterium ions and neutrals is negligible.

In order to reveal an influence of deuterium neutrals on graphite erosion, the target is positively biased (~ +30 V) to avoid the ion bombardment. These experimental data are shown by closed squares in Fig. 7.

The graphite weight loss due to deuterium neutrals has a peak around 700 K. Comparison between the chemical erosions with and without positive basing shows that more than 50% of the chemical erosion is due to deuterium neutral bombardment when the surface temperature is in the range of 600–800 K. This experimental result indicates that the effect of neutral irradiation would be significant even if the neutral temperature is around 0.1 eV.

We need to evaluate erosion yield due to deuterium neutrals; however, we can not evaluate the erosion yield at this moment because it is quite difficult to measure deuterium neutral flux (fluence) in the present experiment. In future, we plan to measure the deuterium neutral density by LIF method with two-photon excitation.

4. Summary

We have investigated the characteristics of detached recombining deuterium plasma in the toroidal divertor plasma simulator, NAGDIS-T. We have produced detached deuterium plasma by controlling the neutral pressure. In the detached plasmas, deuterium Balmer series spectra were clearly observed up to an excited level of ~25 together with the continuum emission associated with radiative recombination. The electron temperature and density in the detached plasmas have been evaluated by optical methods. It is found that the EIR plays a dominant role to form the deuterium detached plasmas at the electron density of around 10^{18} m^{-3} and electron temperature of less than 0.5 eV, while it is also found that MAR process could be a particle loss process when the electron density is less than 5×10^{18} m^{-3}.

Furthermore, we have performed the plasma irradiation experiments to graphite target in the detached deuterium plasmas. It is revealed that neutral particles generated by EIR process could have strong influence on the carbon chemical erosion.

Acknowledgement

This research was supported by the Ministry of Education, Science, Sports and Culture, Grant-in-Aid for Scientific Research (B), 19360413, 2008.

References

[1] N. Ohno et al., J. Nucl. Mater. 337–339 (2005) 35.
[2] M. Nagase et al., J. Nucl. Mater. 363–365 (2007) 611–615.
[3] N. Ohno et al., Nucl. Fus. 41 (2001) 8.
[4] B. Mihaljčič et al., Phys. Plasmas 14 (2007) 013501.
[5] J. Miyazawa et al., Nucl. Fus. 46 (2006) 532.
[6] V.A. Soukhanovskii et al., J. Nucl. Mater. 363–365 (2007) 432.
[7] A. Loarte et al., Nucl. Fus. 38 (1998) 331.
[8] N. Ohno et al., Phys. Rev. Lett. 81 (1998) 818.
[9] D. Nishijima et al., Plasma Phys. Control. Fus. 44 (2002) 597.
[10] E.M. Hollmann et al., Plasma Phys. Control. Fus. 48 (2006) 1165.
[11] S.I. Krasheninnikov, Phys. Scripta. T96 (2002) 7.
[12] A.G. McLean et al., J. Nucl. Mater. 363–365 (2007) 86.
[13] S. Brezinsek et al., J. Nucl. Mater. 363–365 (2007) 1119.
[14] N. Matsui et al., in: Proceedings of ISETS07, 2007.
[15] R.D. Monk et al., J. Nucl. Mater. 241–243 (1997) 396.
[16] N. Ohno et al., Contrib. Plasma Phys. 41 (2001) 473.
[17] H.R. Griem, Principles of Plasma Spectroscopy, Cambridge University, Cambridge, 1997.
[18] D. Nishijima et al., J. Nucl. Mater. 290–293 (2001) 688.
[19] H.R. Griem, Spectral Line Broadening by Plasmas, Academic, New York, 1974. p. 162.
[20] N. Ezumi et al., J. Nucl. Mater. 266–269 (1999) 337.
[21] D. Nishijima et al., Contrib. Plasma Phys. 38 (1998) 55.